

Wear Assessment of Fe-TiC/ZrC Hardfacing Produced from Oxides

S. Corujeira-Gallo^a, N. Alam^a

^aCSIRO - Process Science and Engineering, 71 Normanby Rd, Clayton VIC3168, Australia.

Keywords:

Hardfacing
Metal matrix composite
Optical and Electron microscopy
Hardness
Three-body abrasion

ABSTRACT

The direct conversion of oxides into carbides during plasma transferred arc welding is a promising processing route to produce wear resistant overlays at low cost. In the present study, Fe-TiC and Fe-ZrC composite overlays were produced by carbothermic reduction of TiO₂ and ZrO₂ during plasma transferred arc deposition. The overlays were characterised by optical microscopy, electron microscopy and X-ray diffraction. The microstructure consisted of small TiC and ZrC evenly dispersed in a pearlitic matrix. The Vickers microhardness was measured and low-stress abrasion tests were conducted. The results showed increased hardness and promising wear resistance under low-stress abrasion conditions.

Corresponding author:

Santiago Corujeira-Gallo
University of Birmingham, Metallurgy
and Materials Edgbaston, B15 2TT,
United Kingdom.
E-mail: s.corujeiragallo@bham.ac.uk

© 2015 Published by Faculty of Engineering

1. INTRODUCTION

The in-situ synthesis of composite overlays during hardfacing processes has shown promising results in recent years [1,2]. These overlays are most typically produced by introducing high contents of carbon and carbide forming elements in the powder feed. Titanium, among other elements, shows great potential because of its high affinity with carbon [3]. The carbides formed in-situ exhibit coherent bonds with the matrix, resulting in high wear resistance [4, 5]. More recently, the authors succeeded in introducing TiC in plasma transferred arc overlays by carbothermic reduction of TiO₂ [6]. As opposed to the exothermic and self-sustaining reaction between Ti and C [7,8], the carbothermic reduction of

TiO₂ relies on high heat inputs for the progressive substitution of C for O during deposition. This carbothermic conversion is thermodynamically favourable at high temperature, such as the one developed during plasma transferred arc (PTA) or welding deposition techniques [9]. In a companion study [6], different volume fractions of reinforcing carbides were introduced in this way and the maximum volume fraction of TiC achievable with this method was 15 %.

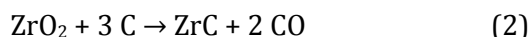
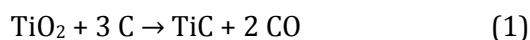
The cost of the metal oxide powder is typically lower than the cost of the metallic or the carbide powders, such as WC [10]. Therefore, this method is expected to produce wear resistant coatings at lower cost, while exhibiting a wear performance suitable for the less-demanding

and less-critical applications. In addition, ZrO₂ and other stable oxides are known to follow a similar reduction path to TiO₂ [11, 12]. Therefore, the present work is a comparative assessment of the microstructure, hardness and wears resistance of Fe-TiC and Fe-ZrC composite overlays produced by carbothermic conversion of TiO₂ and ZrO₂ during PTA deposition.

2. EXPERIMENTAL PROCEDURES

2.1. Powder blends

The metallic powders and powder blends used for this study are listed in Tables 1 and 2, and they consisted of pure iron powder (Hoganas A100S, D50 = 75 µm, of chemical composition as per Table 1) mixed with TiO₂ and ZrO₂. Synthetic rutile with a TiO₂ content of 92 % was selected for the former, while Sigma Aldrich ZrO₂ 99 % pure powder was used for the latter. In both cases, the oxides were mixed with graphite powder in a 4.5:1 molar ratio. This represents a 50 % excess of carbon over the stoichiometric requirement for the carbothermic reactions [12]:



Small quantities of alkali salts were added to the powder blend as catalysts and fluxing agents [6]. The oxide/graphite powder blends were first crushed in a ring mill to a mean particle size of 10 µm, subsequently blended with the pure iron powder, and finally homogenised in a tumble mixer for 4 hours, under dry conditions.

Overlays produced with a white iron alloy by Sandvik, of chemical composition as per Table 1, were used as benchmarks in the wear assessment.

Table 1. Chemical composition of the metallic powders / wt%.

Powder	Fe	Cr	C	Mn	Mo	O	S	P
A100S	Bal.	-	0.4 %	-	-	1.4 %	0.009 %	0.005 %
White iron	Bal.	37 %	3.5 %	1.0 %	0.9 %	-	-	-

Table 2. Composition of the powder blends used for the overlays / wt%.

Powder blend	Fe	TiO ₂	ZrO ₂	C	Na ₂ CO ₃	K ₂ CO ₃	H ₃ BO ₃
Fe-TiC	75 %	15 %	-	8.5 %	0.25 %	-	1.25 %
Fe-ZrC	70 %	-	21 %	8.7 %	-	0.30 %	-

2.1. Deposition conditions

The AISI 1020 substrate plates were cut from a hot rolled bar of rectangular section to a final dimension of (80 x 32 x 10) mm. The plates were ground with #120 emery paper, degreased with acetone and pre-heated to 100 °C before the deposition trials, in order to remove the adsorbed moisture. The overlays were deposited using a Eutectic Castolin GAP 375 plasma transferred arc (PTA) equipment and an E52 torch fitted with a tungsten electrode. The stand-off distance was 8 mm, the arc was established using argon as plasmagene gas, and a mixture of Ar-5 % H₂ as shielding gas. The powder blend was injected into the arc by a fluidised bed powder feeder, using argon as carrier gas, at a flow rate of 15 g/min and 2.0 L/min respectively.

During the deposition process, the torch was oscillated across the width of the sample at a speed of 1.5 m/min, while moved along the longitudinal axis of the sample at a speed of 0.05 m/min. The deposition current was 130 A and two layers were deposited to produce overlays of sufficient thickness (3 mm) for subsequent wear tests. The specimens were cross-sectioned, mounted in epoxy resin, metallographically polished and etched with Nital 2 % to reveal the microstructure.

2.1. Characterisation

Observations were conducted in an Olympus GX71 optical microscope and a Leica S440 scanning electron microscope (SEM) fitted with an Oxford Instruments X-Max energy dispersive X-ray (EDX) detector and Aztec software for chemical analysis. The image analyses were conducted using ImageJ software version 1.45 s, to measure the volume fraction and the size of the precipitates; a minimum of five frames were analysed in order to obtain statistically significant values.

The X-ray diffraction (XRD) traces were collected using the Bragg-Brentano configuration in a Phillips X'Pert system with a cobalt source, and the present phases were identified using X'Pert HighScore software and an ICDD 2012 database.

2.2. Hardness and wear tests

The microhardness was measured with a Buehler Micromet 2100 unit, using a Vickers indenter and applying 100 g load with a holding time of 10 s. A minimum of 8 valid indentations were measured and averaged for each material and the standard deviation was calculated.

Low-stress abrasion wear tests were conducted in triplicates using a dry sand rubber wheel equipment, in accordance with ASTM G65 standard procedure A [13]. The surface of the specimens was ground, to obtain a flat area suitable for the tests. The roughness was measured using a Mahr Perthometer FRW750, to confirm that R_a was below $0.8 \mu\text{m}$ in all cases.

The samples were ultrasonically cleaned with acetone before and after the tests, and the weight loss was measured using a Gibertini Crystal 300CAL balance with ± 0.1 mg accuracy. The volume loss was calculated from the weight loss, using the theoretical density of the material, and the wear coefficient was calculated from the weight loss, the sliding distance and the applied load. The uncoated mild steel substrate and overlays produced with a white iron alloy were also tested, for reference purposes.

3. RESULTS AND DISCUSSION

3.1. Microstructure

Figure 1 shows the typical optical micrographs of the Fe-TiC and Fe-ZrC overlays. Some of the carbon introduced in the powder blend was dissolved in the iron, resulting in a pearlitic matrix. The rest of the carbon was consumed during the carbothermic conversion of TiO_2 and ZrO_2 into TiC and ZrC respectively. Small polygonal and dendritic carbides, evenly dispersed in the matrix, can be seen in Figs. 1 and 2. The SEM backscattered electron (BSE) images in Fig. 2 reveal the composition contrast

between the carbides and the Fe matrix. The TiC appeared darker than the matrix, and the shape of these carbides was mainly polygonal. On the other hand, the ZrC appeared lighter in the image, as it was expected for a phase with larger mean atomic number. At the same time, ZrC exhibited a marked trend toward developing dendritic growth.

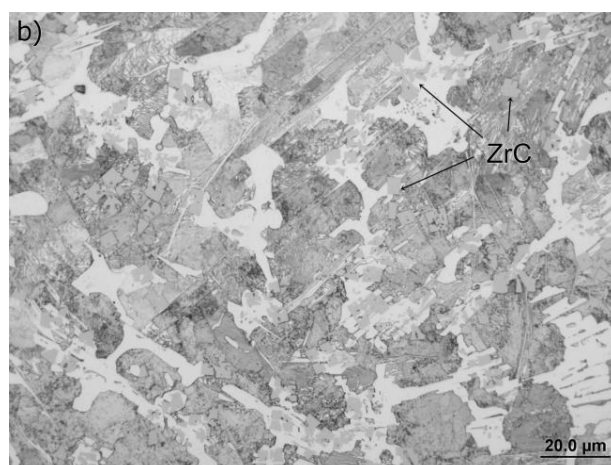
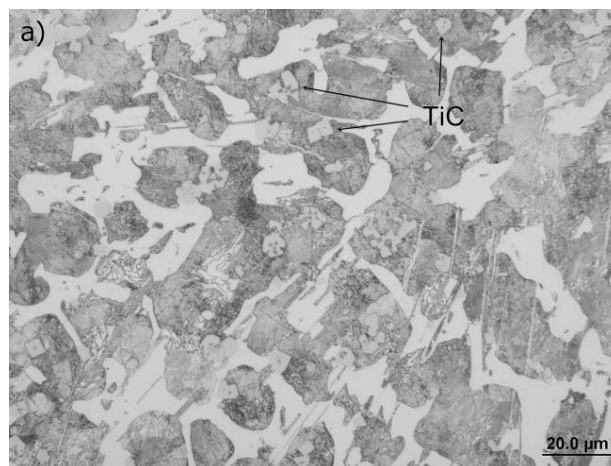
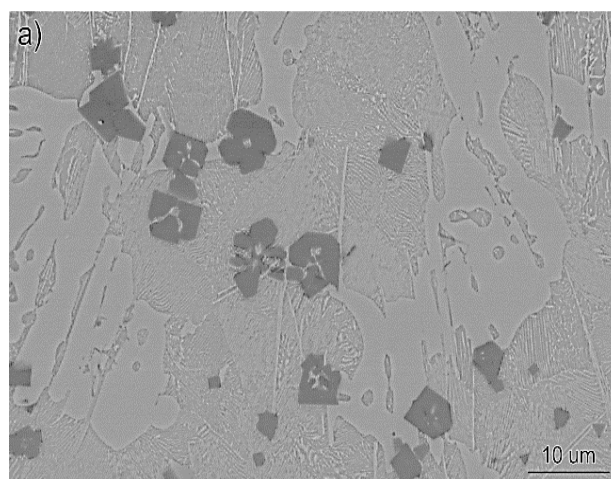


Fig. 1. Optical micrographs of the overlays: a) Fe-TiC and b) Fe-ZrC.



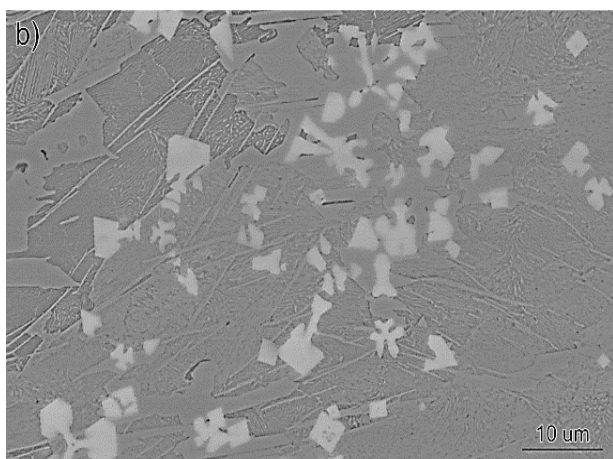


Fig. 2. SEM backscattered electron images of a) Fe-TiC and b) Fe-ZrC overlays.

The X-ray diffraction (XRD) traces were collected from both overlays to identify the present phases. Figure 3 presents the results, where the diffraction peaks corresponding to α -Fe, TiC, ZrC and Fe₃C can be observed. No traces of unreacted oxide or free graphite were identified. These XRD results are in agreement with the observations conducted by optical and electron microscopy. Therefore, the BSE images were analysed further to quantify the volume fraction and the mean size of the carbides.

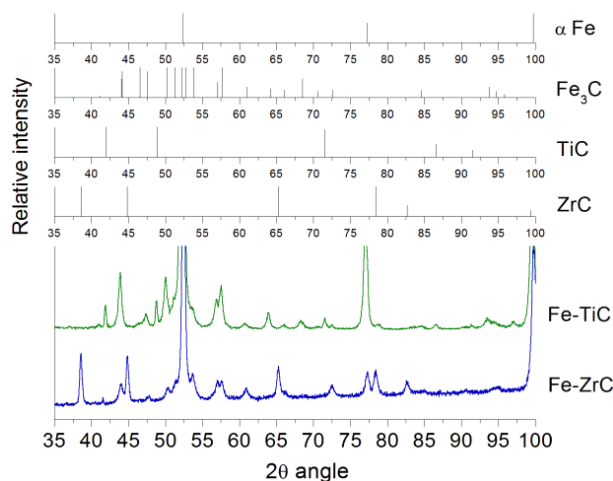


Fig. 3. X-ray diffraction traces from Fe-TiC and Fe-ZrC overlays.

Table 3. Summary of results.

Sample ID	Carbide content [vol-%]	Carbide size [μm]	Carbide morphology	Hardness [HV _{0.1}]	Wear coefficient [μg/m·N]
Fe	-	-	-	166±2	1.6400
White iron	-	-	-	532±40	0.2856
Fe-TiC	10.8 %	7.4 μm	Polygonal	488±29	0.3062
Fe-ZrC	11.9 %	8.6 μm	Dendritic	483±24	0.2907

The characterization of the Fe-TiC and Fe-ZrC overlays revealed very similar results in both cases. Table 3 summarises the volume fraction, mean carbide size, typical carbide morphology, as well as the average microhardness and wear coefficient for each case. The volume fraction of carbides introduced in these overlays was comparable to the maximum achievable using this method [6]. The attempts to introduce larger volume fractions of carbides typically resulted in overlays with high levels of porosity, which was attributed to the CO gas evolved from reactions (1) and (2).

3.2. Wear resistance

The volume loss from low stress abrasion tests is presented in Fig. 4, with mild steel and white iron overlays as reference materials. The experimental results were in agreement with reference data from the ASTM G65 standard [13] and from similar wear assessments [7,8]. The Fe-TiC and Fe-ZrC composite overlays showed a marked increase in wear resistance compared to the mild steel specimens. In both cases, the volume loss and the wear coefficient (Table 3) were comparable to the white iron overlays.

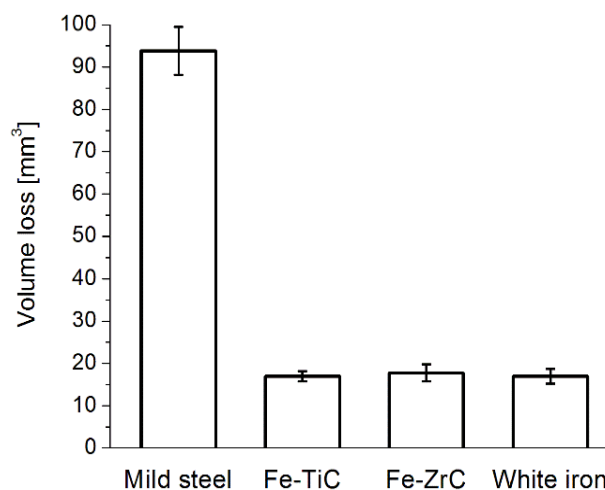


Fig. 4. Volume loss after ASTM G65 low stress abrasion tests.

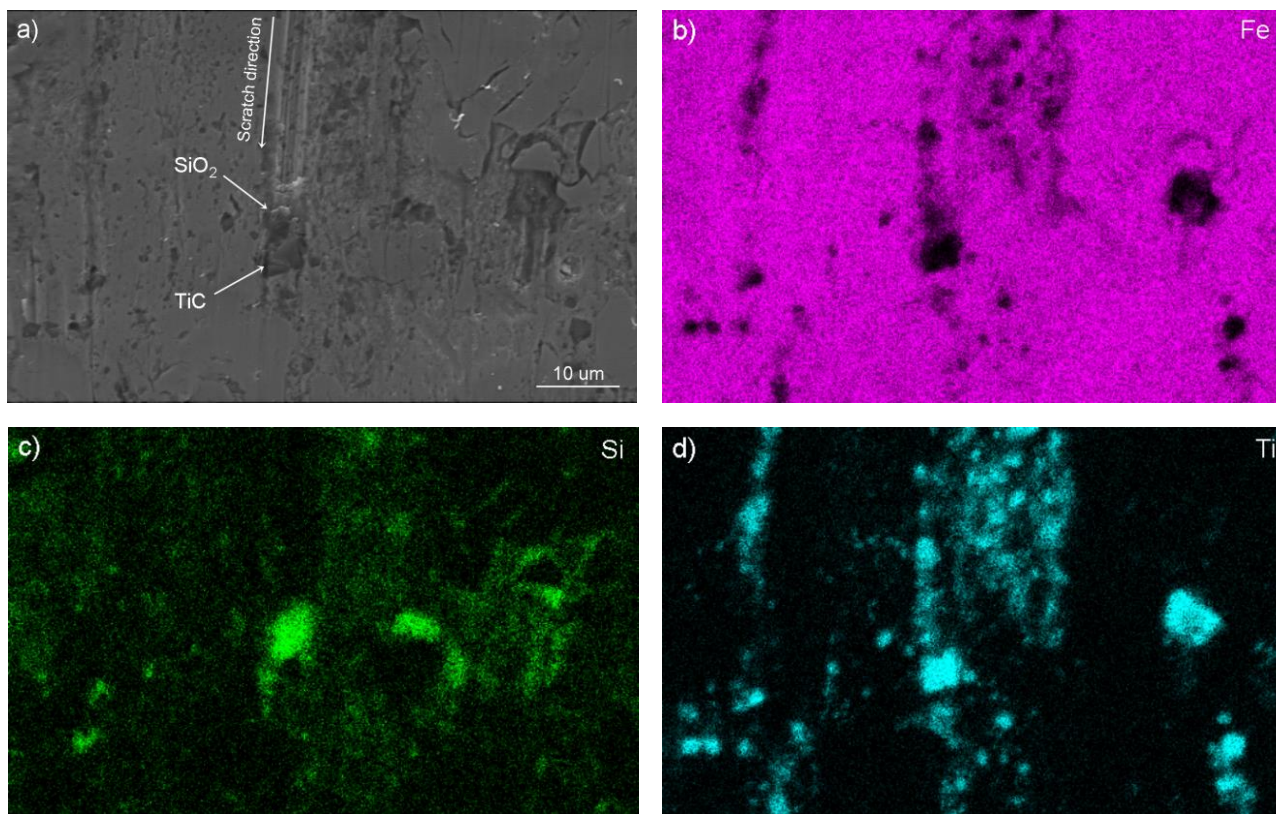


Fig. 5. a) SEM image of the worn surface of a Fe-TiC overlay and EDX composition maps of b) Fe, c) Si and d) Ti.

The wear scars were observed at higher magnification to identify the operating wear mechanisms. The scratches produced by sand abrasive particles (SiO_2) on the harder pearlitic iron matrix of the composite overlays were shorter and shallower than the scratches observed on the softer mild steel reference sample. More importantly, the abrasion scratches on the composite overlays consistently ended at TiC and ZrC precipitates, as it is illustrated by the secondary electron image and the EDX composition maps in Fig. 5. This is a good indication of the high hardness of the carbides and their coherent bond with the matrix.

The wear results obtained in this study are comparable to a wear assessment conducted on Fe-20 vol% TiC overlays produced in-situ from a mixture of Fe, Ti and C powders [5]. This was attributed to three factors, namely: the carbide size, the solution hardening of the matrix and the suppression of intermetallic phases. In first place, the morphology of the TiC produced in the present study was mainly polygonal, with only minor dendritic growth in the case of ZrC. The carbide size was also smaller, thus reducing the mean free path between carbides. Therefore, the uniform distribution of small carbides protected the matrix

against preferential abrasion more efficiently than larger but sparser TiC dendrites. In second place, the excess of carbon, which was introduced in the powder blend for the carbothermic reduction of the TiO_2 and ZrO_2 oxides, had a hardening effect on the iron matrix. As a result, the preferential abrasion of the matrix was reduced even further. Finally, the carbothermic conversion of oxides into carbides proceeds by progressive substitution of C for O in the structure, without formation of elemental zirconium or titanium. This suppressed the formation of intermetallic Laves phases, such as Fe_2Ti , which are associated with brittle-fracture wear mechanisms [5].

In spite of the benefits mentioned in the previous paragraph, higher volume fractions of TiC and ZrC are necessary to increase the wear resistance of these overlays. Unfortunately, this could not be achieved using the current method, without introducing excessive levels of porosity in the overlays. Therefore, it is expected that the methodology described in this study would be suitable for the less-demanding and less-critical applications only. Further developments of this technique are necessary to introduce higher volume fractions of carbides and expand the range of application of these overlays.

4. CONCLUSIONS

The assessment of microstructure, hardness and wear resistance of Fe-TiC and Fe-ZrC composite overlays produced by carbothermic conversion of TiO₂ and ZrO₂ during PTA deposition resulted in the following conclusions:

- Fe-TiC and Fe-ZrC composite overlays can be produced by carbothermic conversion of TiO₂ and ZrO₂ during PTA deposition.
- The microstructure produced in this way consists of small polygonal or dendritic carbides (TiC or ZrC) evenly dispersed in a pearlitic matrix.
- The Fe-TiC and Fe-ZrC composite overlays exhibit promising wear resistance under low stress abrasion conditions.

REFERENCES

- [1] S. Yang, W. Liu, M. Zhong, Z. Wang and H. Kokawa, 'Fabrication of in situ synthesized TiC particles reinforced composite coating by powder feeding laser cladding', *Journal of Materials Science*, vol. 40, no. 9, pp. 2751-2754, 2005.
- [2] X.H. Wang, S.Y. Qu, B.S. Du and Z.D. Zou, 'In situ synthesised TiC particles reinforced Fe based composite coating produced by laser cladding', *Materials Science and Technology*, vol. 25, no. 3, pp. 388-392, 2009.
- [3] V. Lazic, D. Milosavljevic, S. Aleksandrovic, P. Marinkovic, G. Bogdanovic and B. Ndeljkovic, 'Carbide type influence on tribological properties of hard faced steel layer – Part I – Theoretical considerations', *Tribology in Industry*, vol. 32, no. 2, pp. 11-20, 2010.
- [4] X.H. Wang, S.L. Song, Z.D. Zou and S.Y. Qu, 'Fabricating TiC particles reinforced Fe-based composite coatings produced by GTAW multi-layers melting process', *Materials Science and Engineering: A*, vol. 441, no. 1-2, pp. 60-67, 2006.
- [5] A. Emamian, S.F. Corbin and A. Khajepour, 'Tribology characteristics of in-situ laser deposition of Fe-TiC', *Surface and Coatings Technology*, vol. 206, no. 22, pp. 4495-4501, 2012.
- [6] S. Corujeira Gallo, N. Alam and R. O'Donnell, 'In Situ Synthesis of TiC-Fe Composite Overlays from Low Cost TiO₂ Precursors Using Plasma Transferred Arc Deposition', *Journal of Thermal Spray Technology*, vol. 23, no. 3, pp. 551-556, 2014.
- [7] M. Jones, A.J. Horlock, P.H. Shipway, D.G. McCartney and J.V. Wood, 'A comparison of the abrasive wear behaviour of HVOF sprayed titanium carbide- and titanium boride-based cermet coatings', *Wear*, vol. 251, no. 1-12, pp. 1009-1016, 2001.
- [8] M. Jones, A.J. Horlock, P.H. Shipway, D.G. McCartney and J.V. Wood, 'Microstructure and abrasive wear behaviour of FeCr-TiC coatings deposited by HVOF spraying of SHS powders', *Wear*, vol. 249, no. 3-4, pp. 246-253, 2001.
- [9] K. Upadhya, J.J. Moore and K.J. Reid, 'Application of thermodynamic and kinetic principles in the reduction of metal oxides by carbon in a plasma environment', *Metallurgical Transactions B*, vol. 17, no. 1, pp. 197-207, 1986.
- [10] A. Vencl, B. Gligorijević, B. Katavić, B. Nedić and D. Džunić, 'Abrasive wear resistance of the iron- and WC-based hardfaced coatings evaluated with scratch test method', *Tribology in Industry*, vol. 35, no. 2, pp. 123-127, 2013.
- [11] L.M. Berger, W. Gruner, E. Langholf and S. Stolle, 'On the mechanism of carbothermal reduction processes of TiO₂ and ZrO₂', *International Journal of Refractory Metals and Hard Materials*, vol. 17, no. 1-3, pp. 235-243, 1999.
- [12] W. Gruner, S. Stolle and K. Wetzig, 'Formation of CO_x species during the carbothermal reduction of oxides of Zr, Si, Ti, Cr, W, and Mo', *International Journal of Refractory Metals and Hard Materials*, vol. 18, no. 2-3, pp. 137-145, 2000.
- [13] ASTM G65 - 04 (2010), *Standard Test Method for Measuring Abrasion Using the Dry Sand/Rubber Wheel Apparatus*, 2010.